JOURNAL OF CATALYSIS 152, 313–321 (1995)

Studies on Pt_xIn_y Bimetallics in NaY

I. Preparation and Characterization

P. Mériaudeau*,[1] C. Naccache,* A.Thangaraj,* C. L. Bianchi,† R. Carli,† and S. Narayanan‡

*Institut de Recherches sur la Catalyse, 2 Avenue Albert Einstein, 69626 Villeurbanne Cedex, France; †University of Milano, Dipartimento di Chimica Fisica ed Electrochimica, Via Golgi 19, 20133 Milano, Italy; and ‡Catalysis Section, Indian Institute of Chemical Technology, Hyderabad 500007, India

Received March 30, 1994; revised November 18, 1994

Bimetallic Pt_xIn_yNaY samples having a constant platinum loading of 5 wt.% and varying indium content (1 to 5 wt.%) were prepared by ion exchange. The samples were characterized by chemisorption of hydrogen, transmission electron microscopy (TEM), scanning transmission electron microscopy–energy dispersive X-ray (STEM–EDX) analysis, X-ray photoelectron spectroscopy (XPS), and infrared spectroscopy (IR) of adsorbed CO. Pt_xIn_y bimetallics have been found in the NaY support as small (8–20 Å) particles as shown by TEM. H_2 and CO chemisorption studies indicated that the number of Pt surface atoms decreases when the indium loading is increased. XPS results indicated that part of the indium is at zero oxidation state, but there is no evidence for a change in the electronic properties of the platinum.

INTRODUCTION

In the recent past, considerable research effort has been directed towards the preparation and the characterization of metallic (1, 2) or bimetallic particles (2) encaged in zeolites. The catalytic performances of bimetallics are very often superior to those of their monometallic counterparts, especially in avoiding fast deactivation (3). The addition of a reducible but catalytically inactive metal, e.g., Cu (2), Au (4), Sn (5, 6), or Pb (7, 8), to an active metal such as platinum is a way to change the selectivity of the platinum metal. From an industrial viewpoint, PtSn (9) or PtInSn (10) catalysts are effective for dehydrogenation or cyclization reactions; from a fundamental viewpoint, although the literature relating to PtSn is well documented, this is not the case of PtIn catalysts. In this work (Part 1) the formation and the characterization of PtIn bimetallics in NaY zeolites have been studied. In a forthcoming paper, the catalytic properties of these solids as studied through propane dehydrogenation hydrogenolysis and *n*-hexane dehydrocyclization will be discussed.

[1] To whom correspondence should be addressed.

EXPERIMENTAL

1. Preparation of the Catalysts

All solid samples were prepared using NaY zeolite from Union Carbide (Linde LZY52) as a support material. The monometallic PtNaY and the bimetallic Pt_xIn_yNaY samples were obtained by ion exchange. The required quantities of $Pt(NH_3)_4(OH)_2$ and $In(NO_3)_3$ were dissolved in water. A known weight of NaY was added to the metal solution and coexchanged under stirring conditions at 353 K for 24 h. All the samples had the same Pt loading (5 wt.%). The indium content was varied from 1 to 5 wt.% by changing the $In(NO_3)_3$ concentration in the metal solution.

In and Pt contents were analyzed by atomic absorption spectrometry (See Table 1 for sample nomenclature: $Pt_5In_{1.1}NaY$ means Pt = 5 wt.%, In = 1.1 wt.%).

The exchanged zeolite was washed twice with deionized water and dried in air at 353 K overnight. Before characterization, the sample was thermally treated under a flow of O_2 from room temperature to 593 K (ramping 0.2 K/min). After 2 h at 593 K, O_2 was flushed with N_2 and then nitrogen was replaced by H_2, the temperature being increased from 593 to 773 K at 0.5 K/min. After 2 h at 773 K, H_2 was replaced by N_2 and the sample was cooled to room temperature before being stored in a desiccator under argon.

2. Hydrogen Chemisorption

Measurement of hydrogen chemisorption at room temperature was carried out in a volumetric apparatus having a vacuum line and a precision pressure gauge (Texas In-

0021-9517/95 $6.00

struments) to measure the pressure. Before any measurement, the sample was reduced again under hydrogen in a static apparatus having a liquid N_2 trap; this second reduction was performed at 773 K for 2 h and then the sample was outgassed at 773 K (10^{-2} Pa). After cooling the sample to 293 K, H_2 was admitted and the first adsorption isotherm was measured. After evacuation for 15 min at room temperature (P = 0.1 Pa) a second isotherm was measured. The difference between the first and the second isotherm extrapolated to zero pressure gives the amount of strongly chemisorbed hydrogen and the dispersion was calculated assuming that one Pt surface atom chemisorbs one hydrogen atom.

$$D = 2 \times \frac{\text{number of moles of chemisorbed } H_2}{\text{number of moles of Pt}}.$$

3. *Transmission Electron Microscopy (TEM) and Scanning Transmission Electron Microscopy–Energy Dispersive X-Ray (STEM–EDX) Analyses*

A few samples were characterized using transmission electron microscopy. Particle sizes were measured from micrographs obtained with a Jeol 2010 TEM instrument and the composition of the individual particles was studied by using STEM–EDX analysis (VG HB501 apparatus).

4. *X-Ray Photoelectron Spectroscopy (XPS)*

Some samples have been analyzed using a Surface Science Instruments (now Fisons Instruments) XPS spectrometer. Monochromated AlKα radiation (1486.6 eV) was used.

5. *CO Chemisorption Studied by Infrared Spectroscopy*

Samples were pressed into thin wafers (15–20 mg), mounted in a special holder, and introduced into an infrared cell allowing circulation of gases. The samples were re-reduced under a flow of H_2 at 773 K for 2 h and evacuated at this temperature ($p = 10^{-2}$ Pa) before being cooled to room temperature and contacted with CO ($p = 2 \times 10^2$ Pa). The IR spectra were recorded with a Bruker IFS 48 FTIR spectrometer.

RESULTS AND DISCUSSION

Hydrogen Chemisorption

It was checked that, for the sample containing no platinum but only indium (5 wt.%), no hydrogen uptake was observed. It appears from Table 1 that the Pt dispersion of Pt_5NaY sample is close to 1; the addition of indium decreases the dispersion. This decrease could be due either to a surface enrichment of PtIn with In (assuming that PtIn bimetallic particles are formed) and/or to an increase in the particle size of Pt particles due to the presence of indium. Before discussing in more detail the H_2 chemisorption results, we will give some characterization results obtained with different techniques.

TABLE 1

Platinum Dispersion as Measured by Hydrogen Chemisorption

	Dispersion			
Sample[a]	Pt_5	$Pt_5In_{1.1}$	$Pt_5In_{3.1}$	Pt_5In_5
H/Pt	0.98	0.86	0.50	0.40

[a] Pt_5 means Pt_5NaY and Pt_5In_y means Pt_5In_yNaY.

TEM

Micrographs relating to Pt_5NaY, $Pt_5In_{1.1}NaY$, $Pt_5In_{3.1}NaY$, and Pt_5In_5NaY are shown in Fig. 1. It is observed that for the Pt_5NaY sample most of the Pt particles have a diameter of nearly 1 nm. In addition, in very few places particles having nearly 2 nm diameter are observed. For indium-containing samples, the particle size distribution is dependent on the In loading. Thus, for the low In loadings (1.1 and 3.1 wt.%), the particles have an average diameter of 1 nm, as was observed for Pt_5. Particles of 2 to 3 nm diameter are also observed but their population is much smaller than the 1-nm particles. By contrast, the Pt_5In_5NaY sample exhibits a double distribution: a fraction of the particles are still in the 1-nm range and the remainder (much larger than for $Pt_5In_{1.1}NaY$ or $Pt_5In_{3.1}NaY$ samples) have a large size of 3 to 4 nm.

The hydrogen chemisorption results are in qualitative agreement with TEM results and the addition of In to Pt causes a decrease in H/Pt. TEM results indicate that the particle growth is, at least partially, responsible for the H/Pt decrease.

STEM–EDX Analysis

Two samples, $Pt_5In_{1.1}NaY$ and $Pt_5In_{3.1}NaY$, have been studied using this technique.

(*a*) *$Pt_5In_{1.1}NaY$.* Analysis of eight large zones including zeolite grains containing a large number of metallic particles gives an average Pt/In (by weight) of 4.6 compared to 4.6 from chemical analysis, the highest value being 6, the lowest 4.3. These results clearly indicate that on a microscopic scale ($\simeq$0.5 μm) the solid has a homogeneous composition. Analysis of individual particles indicates (Table 2) that the Pt/In values are different from those obtained for large zone analysis.

TABLE 2

Analysis of Large Zones Including a Great Number of Individual Particles and of Individual Small Particles

Nature of the analyzed zones	Number of analyses	Pt/In (wt.%) Averaged value	Pt/In (wt.%) Highest value / Lowest value	Pt/In (wt.%) (chemical analysis)
Large zones	8	4.6	6 / 4.3	4.5
Individual particles	22	27	49 / 14	4.5[a]

[a] It is assumed that all In is incorporated in Pt particles.

(*b*) *$Pt_5In_{3.1}NaY$.* The same type of procedure (analysis of large zones and of individual particles) has been used for $Pt_5In_{3.1}NaY$ sample and the results are reported in Table 3.

From Tables 2 and 3, it appears clearly that the analyses of large zones and of individual particles do not give the same results. The analysis of large zones on both samples gives a Pt/In ratio close to that expected from elemental analysis, indicating a homogeneous composition of the solids at a macroscopic scale. The results obtained from the analysis of individual particles, however, are different. The Pt/In values obtained are larger than expected from elemental chemical analysis. This result can be explained by assuming that indium is forming a highly dispersed In_2O_3 phase or In^{3+} ions in exchange positions located inside the zeolite support and that only a fraction of the total indium has reacted with Pt to form bimetallic particles Pt_5In_y, y being lower than the initial indium loading (see XPS results). Due to the high platinum loading used and due to the high dispersion obtained, it is difficult to find zones of zeolite having no Pt particles. For the $Pt_5In_{1.1}NaY$ sample, it has not been possible to find any zone for STEM–EDX analysis having no Pt particle. However, for the $Pt_5In_{3.1}NaY$ sample, in one place, it was possible to focus the analysis (zone of 3 × 4 nm) on one particle and the Pt/In ratio obtained was 8.1. On enlarging the analysis zone (6 × 8 nm), the Pt/In ratio decreased to 4.8, suggesting that some indium was located on the zeolite support but not in interaction with platinum. Indeed, this information is only qualitative and cannot be used to calculate the fraction of indium which is dispersed through the zeolite support. Examination of 5 wt.% InNaY with TEM (micrograph not given here) reinforces this explanation since the presence of very small particles of indium (or indium oxide) is clearly observed.

To summarize, TEM and STEM–EDX analyses indicate that particles containing platinum and indium are formed, these particles being enriched in Pt with respect to the theoretical value.

TABLE 3

STEM–EDX Analysis of Large Zones Including a Great Number of Individual Particles and of Individual Small Particles

Nature of analyzed zones	Number of analyses	Pt/In (wt.%) Averaged value	Pt/In (wt.%) Highest value / Lowest value	Pt/In (wt.%) (chemical analysis)
Analysis of large zones	8	1.9	2.1 / 1.8	1.6
Analysis of individual particles	19	7.8	12.5 / 6.7	1.6[a]

[a] It is assumed that all indium is forming a bimetallic with Pt.

Infrared Studies of Adsorbed CO

Infrared spectra of adsorbed CO have been employed to give evidence for the formation of bimetallic PtIn particles. For this purpose, the change in the number of bridged CO species per gram of platinum as a function of the indium loading has been considered, together with the shift of ν(CO) relative to the Pt–CO singleton value. It has been assumed, in accordance with previous published work on IR studies of CO adsorbed on Pt alloy particles (11), that the formation of bimetallic PtIn particles will be evidenced by a shift to lower value of ν(CO) (linear Pt–CO) and by a decrease of the IR band intensity corresponding to bridged CO. In Fig. 2 are shown the results of CO absorbance obtained for different samples. In Table 4, the absorbance per gram of platinum for Pt–CO linear species and for bridged species and the ratio Absorbance (bridged species)/Absorbance (linear species) as a function of the indium content are given.

Assuming that the extinction coefficients of these species are unchanged upon addition of indium to platinum,

TABLE 4

IR Absorbance of Pt–CO Species and of Bridged CO Species and Ratio of These Numbers as a Function of the Indium Loading

Sample	Absorbance, A_1[a]	Absorbance, A_2[a]	Bridged/linear species	Pt/CO (linear)[b]
Pt_5NaY	7.9	1	0.126	1
$Pt_5In_{1.1}NaY$	8	0.5	0.062	1
$Pt_5In_{3.1}NaY$	3.8	0.03	0.008	0.5
Pt_5In_5NaY	1.2	0.01	0.008	0.16

Note. A_1, Absorbance of Pt–CO linear species; A_2, absorbance of bridged CO species.

[a] Arbitrary units.

[b] Pt/CO as calculated with values of column 1, assuming that for PtNaY, Pt/CO = 1.

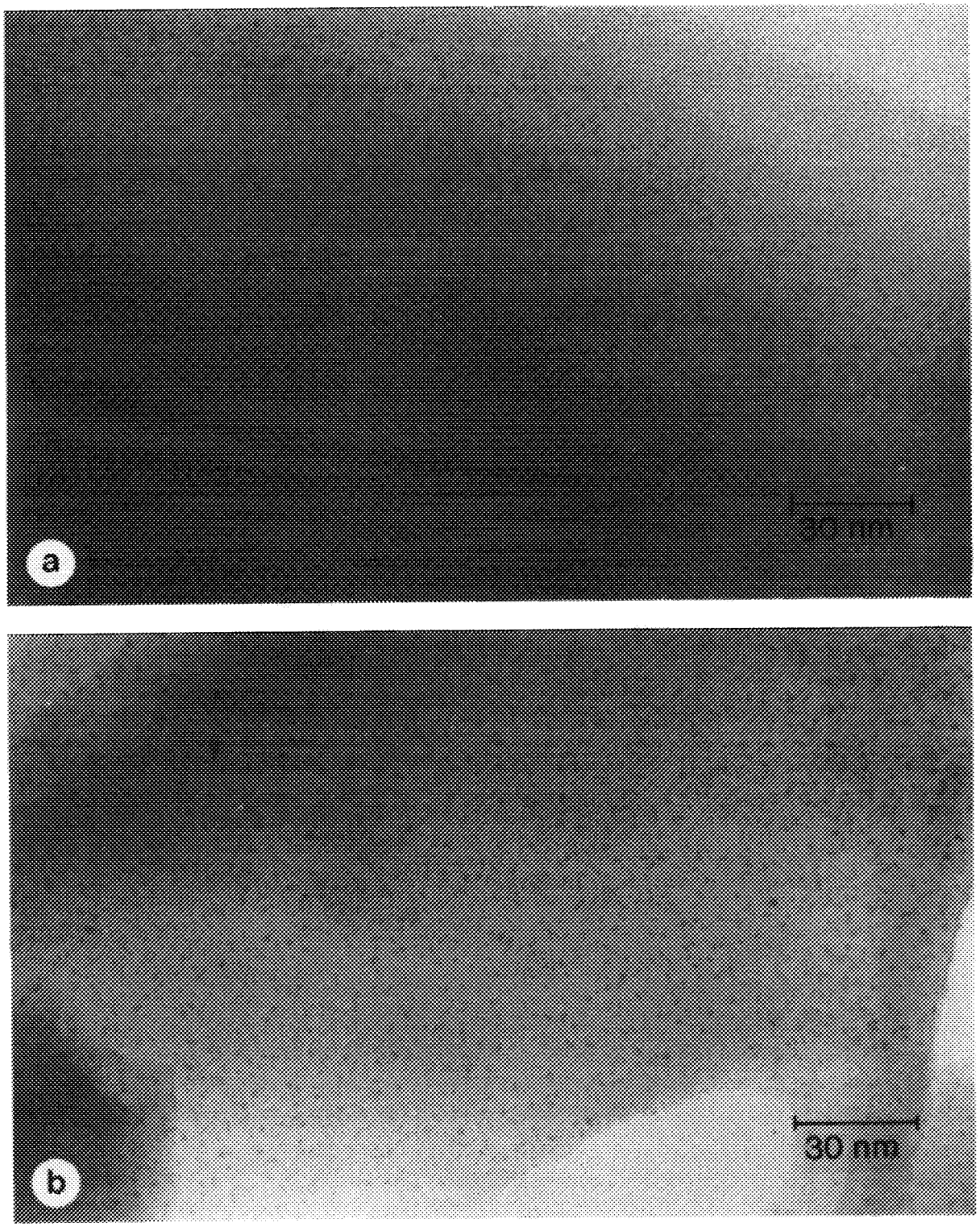

FIG. 1. Micrographs of Pt_xIn_yNaY samples: (a) Pt_5NaY, (b) $Pt_5In_{1.1}NaY$, (c) $Pt_5In_{3.1}NaY$, and (d) Pt_5In_5NaY.

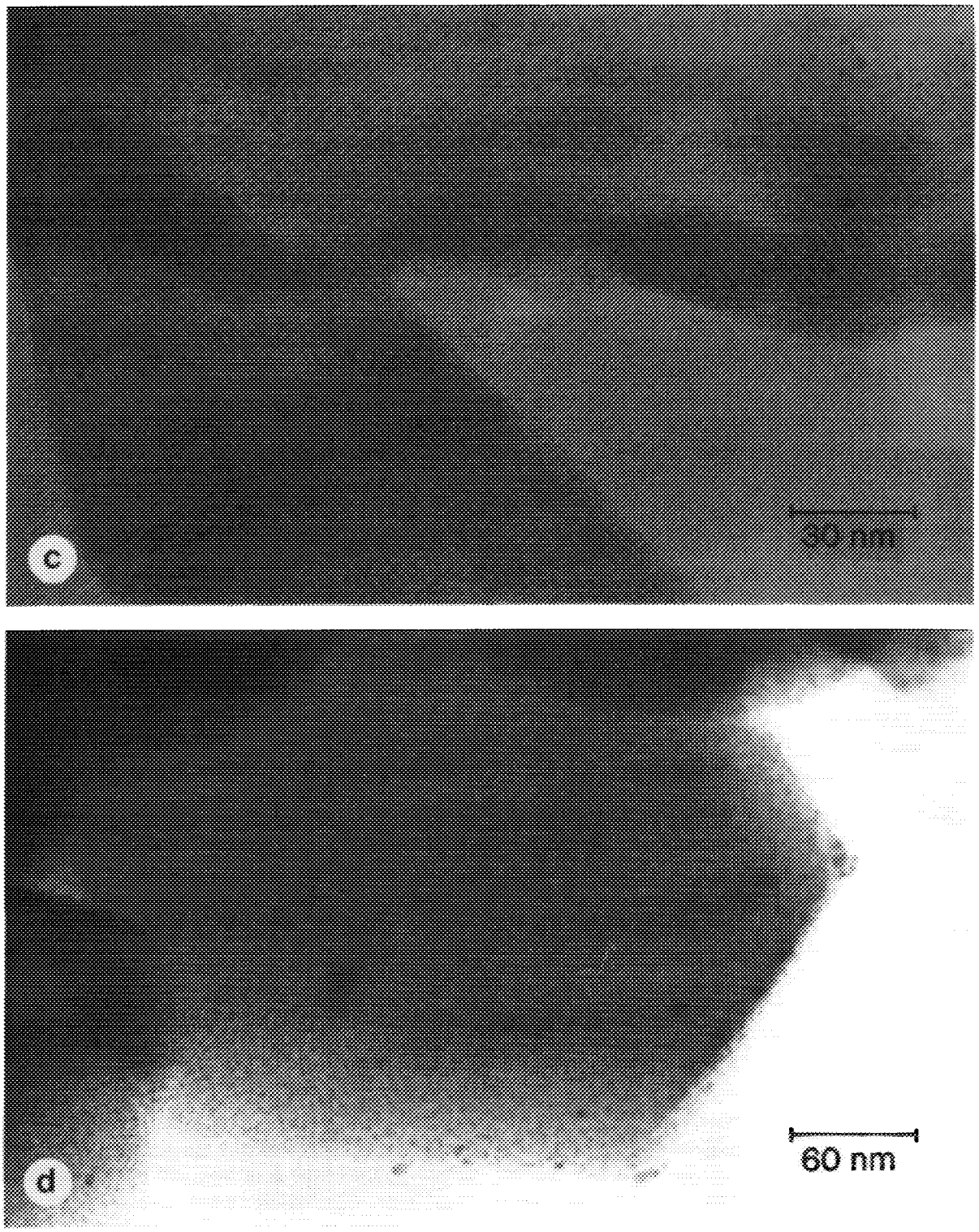

FIG. 1—*Continued*

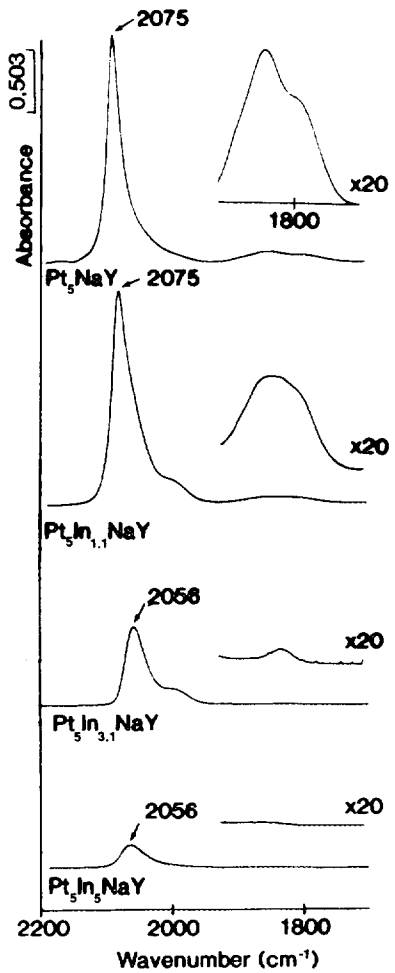

FIG. 2. Infrared spectra of adsorbed CO on Pt_5In_yNaY samples. CO gas phase was removed at 298 K. Absorbance scale is the same for all spectra.

these numbers would correlate with the number of Pt surface atoms. Thus, in the last column of Table 4, the dispersion (Pt/CO) has been calculated taking into account only the Pt–CO linear species.

From Table 4 and Fig. 2, the following three major facts emerge.

(i) The number of CO species per gram of platinum is strongly dependent on the In content; the higher the indium content, the lower the number of adsorbed CO species. In addition it is observed that the linear CO species decreased less than the bridged CO species. These results suggest that the presence of indium prevents CO from forming multiple bonds with Pt atoms because of the dilution effect evidenced previously (11, 12) for other Pt-based alloys.

(ii) At full CO coverage, the ν(CO) singleton wavenumber decreased with the increase of the indium loading, this again suggesting that the dilution effect is operating (12), and consequently CO is much less perturbed by dipolar effects on PtInNaY samples. This is confirmed by desorption studies: desorption at 573 K (1 h) of Pt_5NaY and $Pt_5In_{3.1}NaY$ samples reduced the number of Pt–CO linear species by a factor of 4 for both samples and decreased ν(CO) to 2059 cm^{-1} for Pt_5NaY and to 2051 cm^{-1} for $Pt_5In_{3.1}NaY$ at zero coverage.

Thus, observations (i) and (ii) clearly indicated that indium species are very close to Pt atoms, probably forming bimetallic particles or decorating Pt particles.

(iii) The Pt dispersion, as measured from chemisorbed CO (last column, Table 4), is not really different from that obtained by hydrogen adsorption except for the sample with highest indium loading, for which the chemisorbed hydrogen exceeds that of CO. These results (decrease in H_2 chemisorption or in CO chemisorption as studied by IR spectroscopy) are in agreement with TEM results which indicated an increase in particle size with the addition of indium. Similar results (decrease in H_2 or CO chemisorption) were reported by Balakrishnan and Schwank (11) and by Palazov *et al.* (8) for $PtSn/Al_2O_3$ and by Cheng *et al.* (13) who studied hydrogen adsorption on $PtTe/Al_2O_3$ and $PtSb/Al_2O_3$. Obviously, more experimental work has to be done to explain the discrepancy between the CO and the H_2 behaviour of the highest In-loaded PtNaY sample.

XPS Studies

In order to have information on the ionic state of indium (and on a possible change in the electronic properties of Pt), XPS has been used. Samples utilized are those having been activated and exposed to air (see Experimental). XPS spectra were recorded on

(a) samples outgassed at 773 K for 2 h ($P = 1.3 \times 10^{-3}$ Pa);

(b) samples reduced *in situ* for 90 min under H_2 ($P = 1.01 \times 10^5$ Pa). After each treatment, spectra of Si(2*p*), Al(2*p*) Pt(4*f*), and In(3*d*) were recorded, Si(2*p*) being taken as an internal reference (BE Si2*p* = 103.5 eV).

Figures 3a and 3b related to the $Pt_5In_{3.1}NaY$ sample before and after reduction. A first examination of these figures indicates that XPS spectra relative to Si(2*p*), Al(2*p*), and Pt(4*f*) are not much changed with the thermal treatment (shapes remain the same). However, in contrast, the In(3*d*) peak is modified because of the reducing treatment. This result clearly indicates that there is no inhomogeneous charging effect and hence it will be possible to discuss the changes observed for the In(3*d*) lines. It appears from Table 5 that the Pt/Si and In/Si atomic ratios obtained by XPS are in reasonable agreement with the values obtained by elemental analysis, bearing in mind that XPS reflects more the surface composition than the bulk.

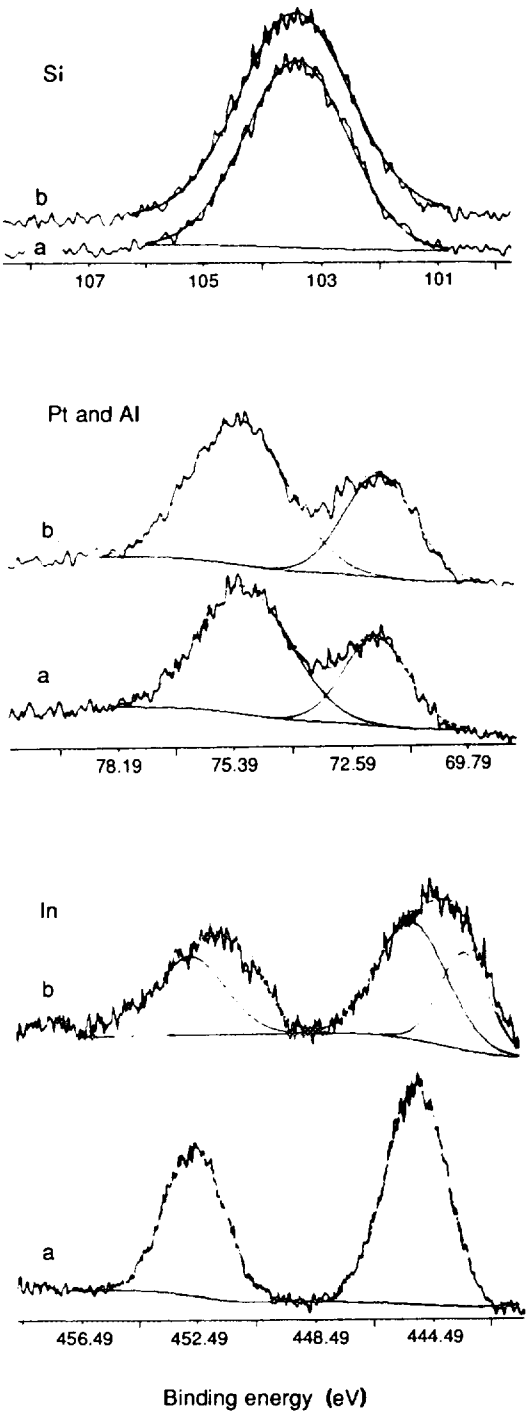

FIG. 3. XPS spectra of $Pt_5In_{3.1}NaY$ outgassed at 723 K (a) and reduced at 723 K under H_2 (b).

Reducing treatment causes a decrease of the In/Pt ratio (Table 5). Since the Pt/Si ratio is almost unchanged, the In/Pt decrease is due to a change of the indium distribution. It is observed that the In/Si ratio decreased significantly. Such a change could be due to the following phenomenon.

TABLE 5

Pt/Si, In/Si, and In/Pt Atomic Ratios as a Function of Thermal Treatment on Different Samples

	Atomic ratio				
	Pt/Si (× 10^2)		In/Si (× 10^2)		
Sample	by XPS[a]	by EA[b]	by XPS[a]	by EA[b]	In/Pt by XPS[a]
Pt_5NaY	1.6 (1.3)	3.6	—	—	—
$Pt_5In_{1.1}NaY$	1.2 (1.1)		0.8 (0.6)		0.75 (0.55)
$Pt_5In_{3.1}NaY$	2.6 (2.4)		8.17 (4.5)		3.16 (2.2)
$In_{4.7}NaY$	—	—	6.8 (3.1)	6	—

[a] After evacuation at 723 K and in parentheses after reduction in H_2 at 723 K.

[b] EA signifies chemical analysis.

TEM and STEM—EDX analyses have shown that Pt and In are forming particles in which both elements are present. For samples having been reduced and contacted with air before outgassing in the XPS spectrometer (Fig. 3a), indium could have segregated on the surface and hence the In/Pt ratio would be higher than in the absence of segregation. In contrast, after the reduction in the XPS chamber (Fig. 3b) indium would have been re-reduced to In^0 (see below) and would have formed a homogeneous bimetallic causing the decrease of In/Pt ratio.

Change in the Oxidation State of Indium and Platinum Due to Reduction Treatment

Table 6 and Fig. 3 indicate that indium exists in two different oxidation states after reduction under hydrogen

TABLE 6

XPS Binding Energies of Pt and In for Samples under Study as a Function of Thermal Treatments

	Binding energies[a] (eV)	
Sample	Pt $4f_{7/2}$	In $3d_{5/2}$
In[b]		443.7 (443.7)
In_2O_3[b]		444.1 (444.1)
Pt_5NaY	71.9 (71.5)	
$Pt_5In_{1.1}NaY$	71.5 (71.2)	445.1 (445.1) (443.8)
$Pt_5In_{3.1}NaY$	71.8 (71.3)	445.1 (445.1) (443.8)
$In_{4.7}NaY$		446.2 (446.2)

Note. Si 2_p (103.5 eV) has been taken as an internal reference for zeolite-based samples.

[a] After evacuation at 723 K and in parentheses after reduction in H_2 at 723 K.

[b] In and In_2O_3 (Johnson Matthey) were etched with argon ions before XPS measurements.

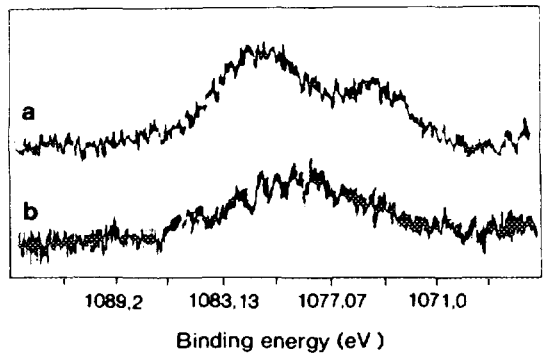

FIG. 4. Auger transitions of indium for $Pt_5In_{3.1}KY$ outgassed at 723 K (a) and reduced at 723 K under H_2 (b).

(BE In_{3d} = 443.8 and 445.1 eV). The part of the indium having the lowest binding energy represents 40% of the total indium content for $Pt_5In_{3.1}NaY$ and nearly 80% for $Pt_5In_{1.1}NaY$. The determination of the oxidation state of indium in the samples using the measured binding energies of the $3d_{5/2}$ levels appears hazardous since, as shown in Table 6 and in agreement with the literature data (14, 15), the shift between In^{3+} (in In_2O_3) and In^0 (In foil) is rather small, viz. 0.4 eV. Generally, the Auger parameter is used to discriminate between In^{3+} and In^0. The Auger parameter is 850.4 eV for In^{3+} and 852.5 for In^0 (15). Unfortunately, with NaY zeolite as a support and an Al$K\alpha$ source, it is not possible to measure the Auger parameter of indium because of the important overlapping of Na_{1s} and In $M_4N_{45}N_{45}$ lines. To overcome this difficulty, despite the fact that all characterization and catalytic studies were performed on PtInNaY samples, Na^+ ions have been exchanged with K^+ in the $Pt_5In_{3.1}NaY$ sample which was reduced and re-exposed to air. For this purpose, the sample was stirred overnight in a 0.1 *M* aqueous solution of K_2CO_3; this treatment was repeated twice at 353 K before the sample was dried in air at 373 K. The spectra of the sample outgassed at 723 K and that obtained after reduction at 723 K are qualitatively identical to those reported in Fig. 3 for low binding energies. However, now, for the unreduced sample, the Auger lines in $M_4N_{45}N_{45}$ are well resolved (Fig. 4a) and the Auger parameter can be evaluated: it is equal to 850.8 eV. In contrast, for the reduced PtInKY sample, the Auger lines are much weaker and broader (Fig. 4b) and it is not possible to calculate the Auger parameter, which strongly suggests that indium species with binding energy at 445.2 and 443.8 eV have different energy Auger transitions causing the broadening of the Auger lines. Since the $Pt_5In_{3.1}KY$ sample (not re-reduced *in situ* but simply outgassed) has a In 3*d* binding energy and an Auger parameter close to that reported for In^{3+}, it is concluded that for both the samples, $Pt_5In_{3.1}KY$ and $Pt_5In_{3.1}NaY$, the indium species are in the same oxidation state In^{3+}. In contrast, after reduction under H_2 at 723 K, a part of the indium In^{3+} (BE = 445.2 eV) is reduced to In^0 (BE = 443.8 eV). The infrared studies of adsorbed CO and STEM–EDX analysis have already shown that Pt and In are in close contact and since a part of the indium is in the zero oxidation state one can suggest that Pt–In bimetallic particles are formed. It is known that Pt and In can form a bimetallic with Pt_xIn_y composition, x/y varying from 0.33 to 2.33 (16). Using values of Tables 5 and 6 and data of Fig. 3, and assuming that all In^0 is present as a bimetallic, one can calculate an In^0/Pt atomic ratio of 1 for the $Pt_5In_{3.1}NaY$ sample and 0.5 for $Pt_5In_{1.1}NaY$; both values are in the expected composition range 0.3 to 2.33. It is observed (Table 6) that the Pt 4f binding energy is slightly lower (0.2 eV) for PtIn than for Pt. Such a small shift could have different origins; namely (i) a change in relaxation effects because of the change in particle size diameters with the addition of indium to platinum and (ii) a change in the electronic properties of Pt due to the alloying with indium. With our data, it is impossible to discriminate between these two causes. Nevertheless, a change in the electronic properties of Pt due to the formation of Pt_xIn_y bimetallic is not unexpected since it has been observed for bimetallics such as PtSn by Balakrishnan and Schwank (17) and PtCr by Joyner *et al.* (18).

CONCLUSIONS

To summarize, these results indicate that the addition of indium to PtNaY and subsequent activation (oxidation and reduction) lead to the formation of PtIn particles. Chemisorption results of H_2 and of CO suggest that the number of Pt surface atoms decreases when the indium content is increased. TEM and STEM–EDX analyses indicate that bimetallic PtIn particles are formed and are Pt enriched. With the addition of indium, a particle growth is observed which correlates with the decrease of H_2 or CO uptake. From XPS results, it is concluded that a fraction of the indium is in the zero oxidation state, responsible for the formation of PtIn bimetallic, the remainder of the indium being in the In^{3+} oxidation state, not in interaction with Pt. Neither XPS results nor IR results gives clear evidence of a possible change in the electronic properties of Pt with the addition of indium.

ACKNOWLEDGMENTS

Mr. Nicot is acknowledged for having made the TEM and STEM–EDX analyses. The Indo–French Center for the promotion of Advanced Research (IFCPAR), New Delhi, India, is acknowledged for funding the project 506-1.

REFERENCES

1. Gallezot, P., *Cat. Rev. Sci. Eng.* **20,** 121 (1979).
2. Sachtler, W. M. H., and Zhang, Z., *Adv. Catal.* **39,** 129 (1993).
3. Sinfelt, J. H., *in* "Catalysis Science and Technology" (J. R. Anderson and M. Boudart, Eds.), Vol. 1, p. 257. Springer, Heidelberg, 1981.
4. Sachtler, J. W. A., and Somorjai, G. A., *J. Catal.* **89,** 35 (1984).
5. Verbeek, H., and Sachtler, W. M. H., *J. Catal.* **42,** 257 (1976).
6. Palazov, A., Bonev, Ch., Shopov, D., Lietz, G., Sárkány, A., and Völter, J., *J. Catal.* **103,** 249 (1987).
7. Bastein, A. G. T. M., Toolenaar, F. J. C. M., and Ponec, V., *J. Catal.* **90,** 88 (1984).
8. Palazov, A., Bonev, Ch., Kadinov, G., Shopov, D., Lietz, G., and Völter, J., *J. Catal.* **71,** 1 (1981).
9. U.S. Patent 4,868,145 (1989) to Mobil.
10. U.S. Patent 4,886,928 (1989) to U.O.P.
11. Balakrishnan, K., and Schwank, J., *J. Catal.* **138,** 491 (1992).
12. Toolenaar, F. J. C. M., Stoop, F., and Ponec, V., *J. Catal.* **82,** 1 (1983).
13. Cheng, C. H., Dooley, K. M., and Price, G. L., *J. Catal.* **116,** 325 (1989).
14. Bertrand, P. A., *J. Vac. Sci. Technol.* **18,** 28 (1981).
15. Pessa, M., Vuoristo, A., Vulli, M., Aksela, S., Vayrynen, J., and Aksela, H., *Phys. Rev. B* **20,** 3115 (1979).
16. Guex, P., and Feschotte, P. J., *Less Common Met.* **46,** 101 (1976).
17. Balakrishnan, K., and Schwank, J., *J. Catal.* **127,** 287 (1991).
18. Joyner, R. W., Shpiro, E. S., Johnston, P., and Tuleuova, G. J., *J. Catal.* **141,** 250 (1993).